Biochimica et Biophysica Acta 1803 (2010) 832–839

Contents lists available at ScienceDirect

Biochimica et Biophysica Acta

journal homepage: www.elsevier.com/locate/bbamcr

ErbB4 regulates the timely progression of late fetal lung development

Washa Liu [a,1], Erkhembulgan Purevdorj [b,1], Katja Zscheppang [b], Dietlinde von Mayersbach [b,c], Jan Behrens [c], Maria-Jantje Brinkhaus [d], Heber C. Nielsen [a], Andreas Schmiedl [c], Christiane E.L. Dammann [a,b,*]

[a] Division of Newborn Medicine, Floating Hospital for Children at Tufts Medical Center, Boston, MA 02111, USA
[b] Department of Pediatric Pulmonology and Neonatology, Hannover Medical School, 30625 Hannover, Germany
[c] Department of Anatomy, Hannover Medical School, 30625 Hannover, Germany
[d] Perinatal Infectious Disease Epidemiology Unit, Hannover Medical School, 30625 Hannover, Germany

ARTICLE INFO

Article history:
Received 12 September 2009
Received in revised form 2 March 2010
Accepted 3 March 2010
Available online 17 March 2010

Keywords:
Transgenic mouse
Surfactant
Lung structure
Inflammation

ABSTRACT

The ErbB4 receptor has an important function in fetal lung maturation. Deletion of ErbB4 leads to alveolar hypoplasia and hyperreactive airways similar to the changes in bronchopulmonary dysplasia (BPD). BPD is a chronic pulmonary disorder affecting premature infants as a consequence of lung immaturity, lung damage, and abnormal repair. We hypothesized that proper ErbB4 function is needed for the timely progression of fetal lung development. An ErbB4 transgenic cardiac rescue mouse model was used to study the effect of ErbB4 deletion on fetal lung structure, surfactant protein (SP) expression, and synthesis, and inflammation. Morphometric analyses revealed a delayed structural development with a significant decrease in saccular size at E18 and more pronounced changes at E17, keeping these lungs in the canalicular stage. SP-B mRNA expression was significantly down regulated at E17 with a subsequent decrease in SP-B protein expression at E18. SP-D protein expression was significantly decreased at E18. Surfactant phospholipid synthesis was significantly decreased on both days, and secretion was down regulated at E18. We conclude that pulmonary ErbB4 deletion results in a structural and functional delay in fetal lung development, indicating a crucial regulatory role of ErbB4 in the timely progression of fetal lung development.

1. Introduction

ErbB receptors play important roles in fetal development [1–4]. ErbB receptors are expressed in fetal lung cells [5] and regulate fetal lung maturation via mesenchyme–epithelial cell communication [6,7]. Their expression in the fetal lung is regulated by a variety of hormones and growth factors [8–10]. The growth factor neuregulin-1, a ligand of ErbB3 and ErbB4 receptors, is secreted by the mature fetal lung fibroblast to stimulate the synthesis of surfactant by lung type II epithelial cells [7]. In the fetal lung, ErbB4 is the most prominent ErbB receptor dimerization partner [5,11]. Silencing of ErbB4 function using siRNA inhibits fetal surfactant synthesis [12]. ErbB4 knockout mice die at about E11 due to cardiac defects [2]. As in utero death coincides with the onset of lung organogenesis, the role of ErbB receptors in late fetal lung development and maturation needs to be elucidated. $HER4^{heart}$ transgenic mice are rescued from their lethal cardiac defects by expressing the human ErbB4 cDNA under the control of the cardiac-specific myosin (α-MHC) promoter. These animals survive fetal development, can reach adulthood, and are fertile. Adult survivors of homozygote (−/−) $HER4^{heart}$ transgenic mice exhibit neural and mammary gland defects [13]. Their lungs show alveolar simplification, airway hyperreactivity, and signs of chronic inflammation [14]. These defects might originate from defective fetal development. Here we present the effects of ErbB4 deletion on late fetal lung development.

2. Materials and methods

2.1. Materials

Rabbit anti-human surfactant protein (SP)-A, rabbit anti-sheep SP-B, rabbit anti-human pro-SP-C, and rabbit anti-mouse SP-D antibodies were from Chemicon Europe (Hofheim, Germany); rabbit polyclonal ErbB4 (C-18) antibody was from Santa Cruz Biotechnology Inc. (Santa Cruz, CA); mouse monoclonal anti-actin clone AC-40 was from Sigma (Hamburg, Germany); goat anti-rabbit IgG (HRP-labelled) and goat anti-mouse IgG (HRP-labelled) were from Zymed Laboratories Inc. (South San Francisco, CA);

Abbreviations: BPD, Bronchopulmonary dysplasia; DCt, Difference in threshold cycle; DSPC, Disaturated phosphatidylcholine; E, Embryonic day; SP, Surfactant protein; $HER4^{heart-/-}$, Homozygote ErbB negative transgene; $HER4^{heart+/-}$, Heterozygote transgene

* Corresponding author. Division of Newborn Medicine, Floating Hospital for Children at Tufts Medical Center, Boston, MA 02111, USA. Tel.: +1 617 636 8738; fax: +1 617 636 4233.
E-mail address: cdammann@tuftsmedicalcenter.org (C.E.L. Dammann).

[1] Both authors contributed similarly to the manuscript.

0167-4889/$ – see front matter © 2010 Published by Elsevier B.V.
doi:10.1016/j.bbamcr.2010.03.003

Precision Plus Protein™ standards (Dual color) were from Bio-Rad Laboratories (Munich, Germany); protran nitrocellulose transfer membrane was from Schleicher & Schuell BioScience (Dassel, Germany); Western Lightning Chemiluminescence Reagent Plus (enhanced chemiluminescence, ECL) and methyl [^{3}H]-choline chloride (specific activity 86 Ci/mol) were from Perkin Elmer/Life Sciences (Boston, MA).

2.2. HER4^{heart} animals

HER4^{heart} transgenic mice were kindly provided by Carmen Birchmeier in agreement with Martin Gassmann. Animals were housed in the animal facilities of Hannover Medical School and Tufts University under pathogen-free conditions. The animal protocols were approved by the institutional IACUC authorities at both institutions. Animal experiments were performed using fetal E17, and E18 HER4^{heart} mice from heterozygote breedings. Genotyping was performed as previously described [14].

2.3. Fibroblast preparation

Pregnant mice were anesthetized, fetuses removed by C-section, and kept in PBS on ice. The E17 fetal lungs were removed, pooled according to genotype +/+ and −/−, minced into 1 mm^3 pieces and dissociated in Hanks buffered saline solution (HBSS) containing DNase (20 μg/ml) and 0.25% trypsin at 37 °C for 10 min. The dissociation was stopped by adding DMEM with 10% fetal calf serum (FCS). The cells were filtered through a sterile 45-μm cell strainer and centrifuged at 650×*g* for 10 min at 4 °C. The cell pellets were resuspended in DMEM with 10% FCS and cells were plated at 6×10^6/dish in 100 mm^2 culture dishes for 60 min at 37 °C to allow for lung fibroblast adherence. The non-adherence cells were washed away. The fibroblasts were cultured until confluence and analyzed for ErbB4 receptor expression.

2.4. Tissue processing

Fetal lungs were obtained and similarly divided into 3 pieces. One part was fixed in 4%PFA, 0.1% GA in 0.2 M HEPES buffer, pH 7.35 for 2 h, washed with 0.2 M HEPES buffer 6 times for 10 min, incubated in sucrose solution overnight at 4 °C, and frozen for morphometric and immunohistochemical analyses. The remaining two parts were snap-frozen in liquid nitrogen, stored at −80 °C and used for protein and RNA isolation. In additional experiments organotypic lung cultures were prepared from individual fetuses, grown on grids at the air liquid interface and used to study surfactant synthesis and secretion.

2.5. Stereological analysis

Stereological analyses were carried out on a Nikon Eclipse 80i microscope (Tokyo, Japan) using the Stereo Investigator Version 6 software (MicroBrightField Inc., Vermont, USA). Three serial hematoxylin–eosin stained cryostat sections (thickness 6 μm, interval 40 μm) from each animal were analyzed using a grid of test points and cycloid lines. Morphometric parameters, including the surface density and volume density of the saccules and their septae, the arithmetic barrier thickness of septae, and the size of the saccules were calculated in E18 lungs. In E17 lungs, the thickness and the volume density of the septal tissue, the volume density of the airspace, the surface density of the saccules or the canalicules, and the size of the saccules or the canalicules were also calculated. This was performed according to the point and intersection counting method [15,16] as previously described [14].

2.6. Western blot of surfactant protein expression

Western blot analyses of frozen fetal lungs for SP-A, SP-B, SP-C, and SP-D expression were performed as described previously [14]. Protein expression was quantified by densitometric evaluations for all experiments.

2.7. Immunohistochemistry of surfactant proteins

Immunohistochemistry of lung cryosections for SP-A, SP-B, SP-C, and SP-D was performed as described previously [17], with minor modifications. Briefly, 6-μm-thick sections were blocked with 3% H_2O_2/PBS-solution and 5% goat serum, incubated for 15 min in an Avidin/Biotin Blocking Kit (SP-2001, Vector Laboratories, Burlingame, USA), and stained with rabbit anti-human surfactant protein (SP)-A, rabbit anti-sheep SP-B, rabbit anti-human pro-SP-C, and rabbit anti-mouse SP-D antibodies (Chemicon Europe, Hofheim, Germany) overnight at 4 °C. Staining with the biotin-conjugated affinity purified goat anti-rabbit IgG (Chemicon International Inc. Europe, Hampshire, UK) was followed by incubation in peroxidase-conjugated streptavidin (Jackson ImmunoResearch Europe Ltd., Newmarket, Suffolk, UK) for 30 min. Then sections were incubated in DAB (diaminobenzidine) solution for 10 min, rinsed in PBS/Tween, dehydrated in ascending series of ethanol, and mounted in Entellan (Entellan Neu, Merck KGaA, Darmstadt, Germany).

2.8. Surfactant protein mRNA expression

Real-time PCR for SP-A, SP-B, SP-C, and SP-D mRNA was performed as previously described [14]. Actin was used as an internal control to normalize the surfactant protein cDNA levels. The relative expression of SP mRNA was calculated using the Ct method. The amount of SP mRNA relative to actin was expressed as $2^{-\Delta Ct}$. Relative SP mRNA expression of HER4$^{heart-/-}$ animals was compared to the mRNA expression of their litter-specific HER4$^{heart+/-}$ control animals and presented as % of the control values.

2.9. Surfactant lipid synthesis (^{3}H-choline incorporation and secretion)

Fetal lung organotypic cultures were prepared from individual fetuses as previously described [18], cultured in DMEM with 10% fetal bovine serum for 48 h, and treated with 0.5 μCi/ml ^{3}H-choline for the following 24 h. The media of the cultures were collected for surfactant lipid secretion analysis. The culture tissue was homogenized and sonicated in ice cold PBS for surfactant lipid incorporation analysis. Aliquots in duplicate were used for protein determination. Following lipid extraction with chloroform and methanol, disaturated phosphatidylcholine (DSPC) was isolated by osmium tetroxide, and separated by thin-layer chromatography on silica gel H chromatography sheets as previously published [7,12]. The resulting spots were scraped into scintillation fluid, counted in a beta scintillation counter, expressed as disintegrations per minute per μg protein, and normalized as percent of experiment-specific controls (HER4$^{heart+/-}$ littermate lungs).

2.10. Immunohistochemistry of inflammatory cells

Immunostaining with CD11b antibodies was performed in 6-μm-thick cryosections as described previously [19]. The procedures and reagents were similar to the immunostaining of surfactant proteins with the exception that the primary antibody was rabbit anti-mouse CD11b (IgG2b, Clone M1/70.15, MorphoSys AbD GmbH, Düsseldorf, Germany; 1:100 in PBS/Tween) antibody. Two to three serial staining sections (interval 40 μm) were evaluated using a light microscope (Nikon Eclipse 80i fluorescence microscope, Nikon GMBH Duesseldorf, Germany). For each section, 300–400 test fields (size of the test frame: 100×100 μm) were evaluated with a constant interval of

400 μm between the test fields in both the *x*- and *y*-axes using a stereo investigator system (MicroBrightField, Inc. Williston, Vermont, USA). Cell densities of neutrophils and macrophages were evaluated after counting the CD11b positive cells in the lung parenchyma and were expressed as cell number per mm^2 (cell density) using the following formula:

$$Q/mm^2 = \frac{number \times grid\ size\ (400 \times 400\ \mu m)/test\ frame(100 \times 100\ \mu m) \times 1,000,000}{area\ of\ interest}$$

$$(Q/\ =\ number\ of\ counted\ cells)$$

2.11. Statistics

Data are presented as mean values ± SEM, if not indicated otherwise. *N* indicates the number of fetal lungs studied. Statistical significance was considered for *p*-values <0.05 using the Student's *t*-test for those data following a normal distribution, and the Mann–Whitney *U* test otherwise.

3. Results

3.1. ErbB4 expression

We confirmed that E17 HER4$^{heart-/-}$ fibroblasts did not express ErbB4 receptor, while ErbB4 was expressed in HER4$^{heart+/+}$ fibroblasts (Fig. 1). The lack of ErbB4 expression in the HER4$^{heart-/-}$ fibroblasts is in agreement with the report of Tidcombe et al. who found in this model that ErbB4 mRNA is expressed only in heart but not in other organs such as brain, liver and mammary gland [13]. We have previously reported that ErbB4 is normally expressed in late gestation wild type fetal rat fibroblasts and type II cells and in fetal mouse type II cells and the mouse MLE12 type II cell line [5,10,11]. We have also found that ErbB4 immunostaining is present in fibroblast clusters neighboring developing saccules and in occasional clusters of columnar airway epithelium of late gestation mouse lungs (unpublished data).

3.2. Lung morphology

Morphometric analyses of E18 lungs showed a significant decrease in the size of saccules to 91.78 ± 2.92% ($p = 0.04$) in fetal HER4$^{heart-/-}$ lungs ($N = 13$) compared to the lungs of their control HER4$^{heart+/-}$ littermates ($N = 12$) (Table 1). More dramatic changes were observed at E17 in the lung structure of transgenic mice (Table 2). Most HER4$^{heart-/-}$ lungs corresponded to the canalicular stage of lung development at E17, whereas control lungs had appropriately progressed to the saccular stage (Fig. 2A–D). These changes in the HER4$^{heart-/-}$ lungs were confirmed quantitatively. The thickness and the visual volume density of the septal tissue were significantly increased (122.74 ± 6.58%, $p = 0.016$ and 122.23 ± 3.5%, $p < 0.001$ respectively), while the volume density of the airspace (73.71 ± 3.92%, $p < 0.001$), and the size of the saccules and canalicules (71.77 ± 3.7%, $p < 0.001$) were significantly decreased in HER4$^{heart-/-}$ lungs ($N = 9$) compared to their HER4$^{heart+/-}$ littermate controls ($N = 6$) (Table 2). These results suggested that deletion of ErbB4 simplifies lung structure and delays alveolar development in the late fetal period.

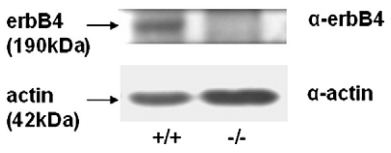

Fig. 1. Representative Western blot of ErbB4 expression in freshly isolated primary E17 fibroblasts of HER4$^{heart+/+}$ (left panel) and HER4$^{heart-/-}$ (right panel) lungs, confirming the deletion of ErbB4 in HER4$^{heart-/-}$ lungs.

3.3. Surfactant protein and mRNA expression

The expression of all four surfactant proteins was analyzed by Western blot and by quantitative real time PCR. At E17, SP-A protein was not changed (133 ± 24%, $N = 7$, $p = 0.2$) and SP-A mRNA level was significantly decreased (50 ± 5%, $N = 7$, $p = 0.03$) in HER4$^{heart-/-}$ lungs compared to HER4$^{heart+/-}$ control lungs (100 ± 3%, $N = 5$; 100 ± 22%, $N = 5$, respectively) (Fig. 3A). At E18, SP-A protein expression was not changed (111 ± 4%, $N = 11$, $p = 0.15$), but SP-A mRNA was significantly increased (141 ± 16%, $N = 10$, $p = 0.03$) compared to HER4$^{heart+/-}$ control lungs (100 ± 6%, $N = 11$; 100 ± 11%, $N = 12$, respectively) (Fig. 3B). SP-B protein was not changed (90 ± 7%, $N = 12$, $p = 0.2$), but SP-B mRNA was significantly decreased (64 ± 7%, $N = 9$, $p = 0.04$) at E17 in HER4$^{heart-/-}$ lungs compared to HER4$^{heart+/-}$ control lungs (100 ± 4%, $N = 8$; 100 ± 13%, $N = 4$, respectively) (Fig. 3C). At E18, SP-B protein was significantly decreased (76 ± 7%, $N = 15$, $p = 0.02$), but SP-B mRNA was now normal (158 ± 46%, $N = 14$, $p = 0.3$) when compared to HER4$^{heart+/-}$ control lungs (100 ± 7%, $N = 13$; 100 ± 26%, $N = 14$, respectively) (Fig. 3D). SP-C was not changed at either the protein (101 ± 9%, $N = 12$, $p = 0.9$) or mRNA level (75 ± 18%, $N = 10$, $p = 0.4$) at E17 in HER4$^{heart-/-}$ lungs compared to HER4$^{heart+/-}$ control lungs (100 ± 2%, $N = 8$; 100 ± 38%, $N = 6$, respectively) (Fig. 3E). At E18 SP-C was lower at the protein level (84 ± 6%, $N = 12$, $p = 0.07$) but higher at the mRNA level (122 ± 21%, $N = 13$, $p = 0.6$) compared to HER4$^{heart+/-}$ lungs (100 ± 5%, $N = 8$; 100 ± 18%, $N = 14$ respectively) (Fig. 3F). However none of these differences were significant. Thus, SP-C was overall not affected in fetal HER4$^{heart-/-}$ mice. At E17, both SP-D protein (173 ± 62%, $N = 7$, $p = 0.3$) and SP-D mRNA (195 ± 64%, $N = 8$, $p = 0.3$) appeared elevated in HER4$^{heart-/-}$ lungs compared to HER4$^{heart+/-}$ control lungs (100 ± 6%, $N = 5$; 100 ± 33%, $N = 6$, respectively). However, these increases did not reach statistical significance (Fig. 3G). At E18, SP-D protein was significantly decreased (78 ± 6%, $N = 15$, $p = 0.014$), but SP-D mRNA was not changed (111 ± 23%, $N = 13$, $p = 0.2$) compared to HER4$^{heart+/-}$ control lungs (100 ± 6%, $N = 13$; 100 ± 16%, $N = 12$, respectively) (Fig. 3H).

3.4. Immunohiostochemestry of surfactant proteins

Immunohistochemistry for SP-A, SP-B, SP-C, and SP-D did not show significant differences in the location of surfactant protein expression (data not shown). Staining for SP-B was detected in Clara cells and in developing type II cells of E18 HER4$^{heart+/-}$ (A) and HER4$^{heart-/-}$ (B) fetal lungs (Fig. 4).

Table 1
Morphometric parameters in the lungs of E18 HER4$^{heart-/-}$ mice compared with control HER4$^{heart+/-}$ mice.

Morphometric parameters	% of litter-specific control	*p* value
Volume density of parenchyma	100.44 ± 0.39	0.35
Volume density of non parenchyma	92.85 ± 8.84	0.22
Thickness of saccular septa	94.39 ± 2.6	0.10
Volume density of saccular septa	98.46 ± 2.42	0.76
Volume density of saccular space	95.73 ± 3.02	0.46
Surface density of saccules	105.01 ± 2.83	0.23
Size of alveolar saccules	91.78 ± 2.92	0.04*
Volume density of ductal space	104.39 ± 6.0	0.70
Size of alveolar ducts	95.18 ± 3.83	0.45
Volume density of ductal septa	108.51 ± 4.67	0.17
Thickness of alveolar ductal septa	102.11 ± 3.27	0.68

Data presented as mean (%) ± SEM.
* $p < 0.05$.

Table 2
Morphometric parameters in the lungs of E17 HER4$^{heart-/-}$ mice compared with control HER4$^{heart+/-}$ mice.

Morphometric parameters	% of family specific control	*p* value
Thickness of septal tissue	122.74 ± 6.58	0.016*
Volume density of septal tissue	122.23 ± 3.50	<0.001*
Volume density of airspace	73.71 ± 3.92	<0.001*
Surface density saccules/canalicules	104.01 ± 4.42	0.91
Size saccules/canalicules	71.77 ± 3.70	<0.001*

Data presented as mean (%) ± SEM.
* $p<0.05$.

3.5. Surfactant lipid synthesis and secretion

3H-Choline incorporation into disaturated phosphatidylcholine (DSPC), a measure of surfactant phospholipid synthesis, was significantly decreased to 64.7 ± 7.6% ($N=4$) in E17 HER4$^{heart-/-}$ lungs compared to HER4$^{heart+/-}$ lungs ($N=9$) ($p=0.008$) (Fig. 5A), and to 50.9 ± 11.5% ($N=5$) in E18 HER4$^{heart-/-}$ lungs compared to HER4$^{heart+/-}$ lungs ($N=14$) ($p=0.0012$) (Fig. 5B). Surfactant secretion, measured as ^{3}H-labelled DSPC content in the culture media, was significantly decreased only in E18 HER4$^{heart-/-}$ lungs to 51.6 ± 9.8% ($N=5$) compared to HER4$^{heart+/-}$ lungs ($N=14$) ($p=0.011$), (Fig. 5B). At E17 this did not reach statistical significance (HER4$^{heart-/-}$ lungs 65.4 ± 23.6%, $N=4$ compare to HER4$^{heart+/-}$ lungs 100 ± 21.8%, $N=9$, $p=0.36$) (Fig. 5A).

In summary, deletion of ErbB4 disturbs pulmonary surfactant homeostasis by down regulation of SP-B and SP-D expression and surfactant phospholipid synthesis and secretion in the late gestation lung.

3.6. Inflammatory cells in the lung

Immunohistochemistry for CD11b showed an increase in inflammatory cells in E17 and E18 HER4$^{heart-/-}$ lungs (Fig. 6A). Cell density of CD11b positive cells was significantly increased to 291.2 ± 58.4 ($p=0.005$) and 47.1 ± 7.6 ($p=0.0017$) cells/mm^2 at E17 and E18, respectively in HER4$^{heart-/-}$ lungs ($N=7$) compared to HER4$^{heart+/-}$ controls (84.3 ± 14.82 and 15.3 ± 2.3 cells/mm^2, respectively; $N=7$) (Fig. 6B-a,b). This leads to the conclusion that deletion of ErbB4 interferes with the development of the innate pulmonary immune system, triggering a chronic inflammatory response.

4. Discussion

Pulmonary deletion of ErbB4 resulted in an overall delay in the timely progression of fetal lung development. Delayed structural

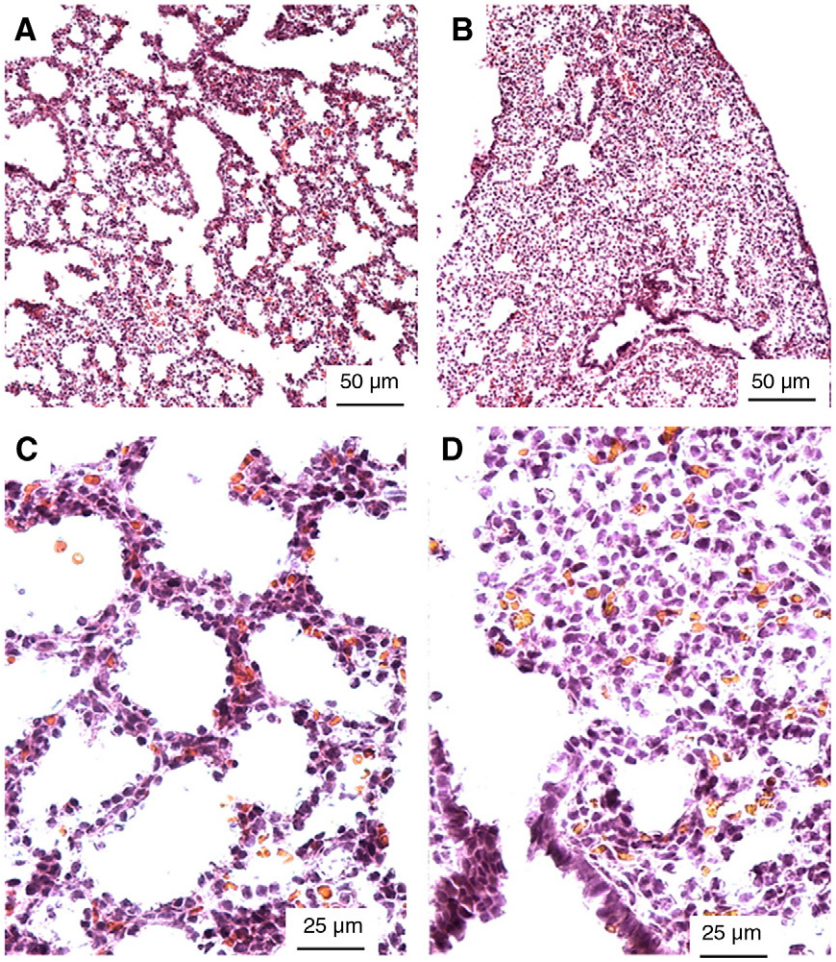

Fig. 2. Histological pictures of E17 control HER4$^{heart+/-}$ (A, C) and HER4$^{heart-/-}$ (B, D) lungs. Representative light microscopic images from cryosections stained with hematoxylin and eosin. HER4$^{heart-/-}$ (B) lungs have fewer transitory ducts and saccules compared to HER4$^{heart+/-}$ control lungs (A). A higher resolution shows more epithelial cells surrounding the air spaces in control lungs (C). HER4$^{heart-/-}$ (D) lungs have less sacculi and show accumulation of tissue containing mesenchyme cells. Morphometric evaluations revealed an increased volume density of the septal tissue and a decreased volume density of the airspace in HER4$^{heart-/-}$ lungs.

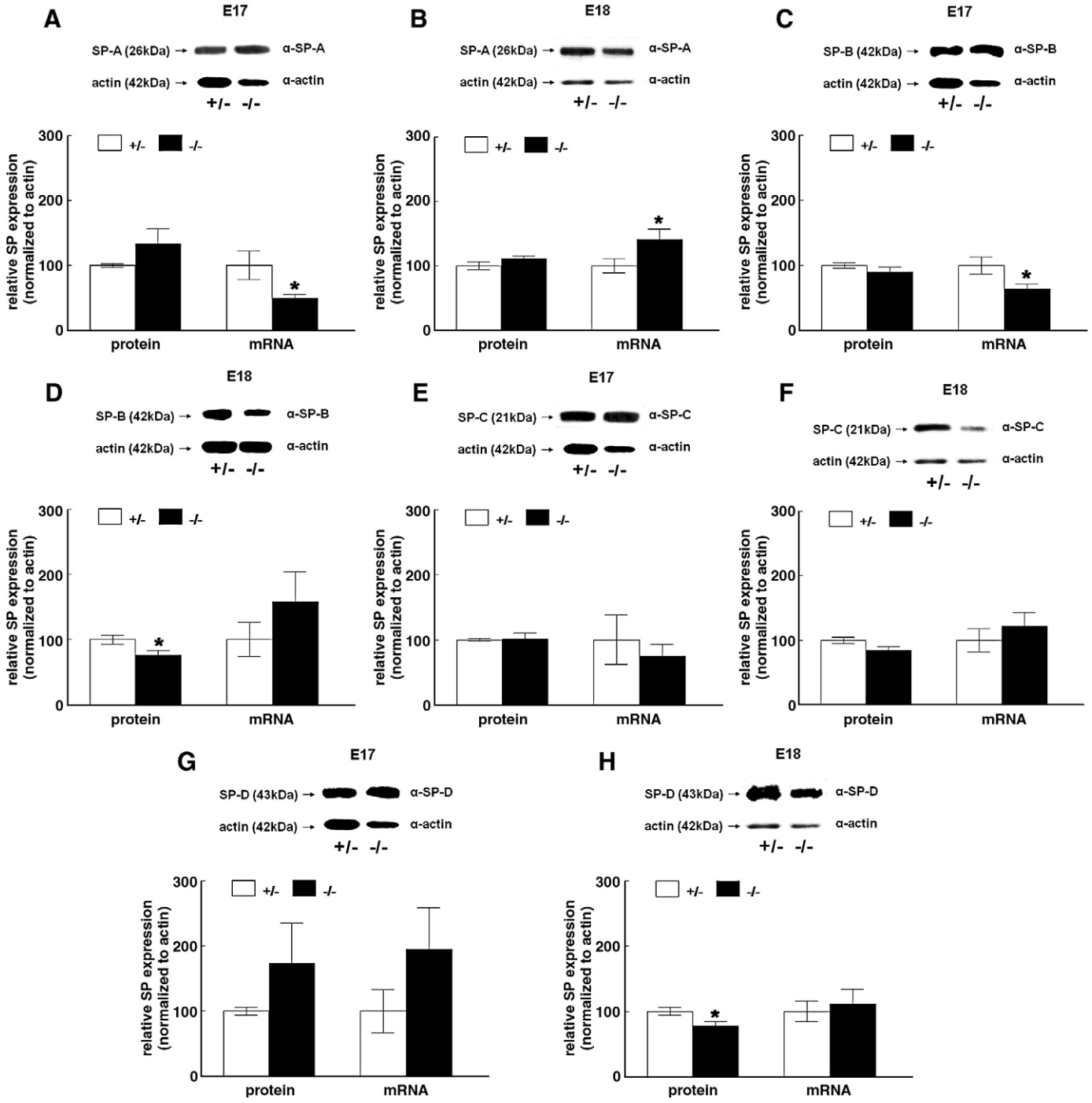

Fig. 3. SP expression. SP-A, SP-B, SP-C, SP-C, and protein expression in E17 (A, C, E, G, respectively) and E18 (B, D, F, H, respectively) lungs. Representative Western blot from HER4$^{heart+/-}$ (left) and HER4$^{heart-/-}$ (right) lung homogenates. Quantification of protein (left) and mRNA (right) expression in lung homogenates from HER4$^{heart+/-}$ (white bars) and HER4$^{heart-/-}$ (black bars) transgenic mice. Values are presented as mean ± SEM, $N = 4$, *: $p < 0.05$.

development was clearly seen in the E17 HER4$^{heart-/-}$ fetal lungs, the stage when the lungs normally advance from the canalicular to the saccular stage. Some catch-up in structural development was observed, as there were less obvious changes in the anatomic structure of the ErbB4-deleted lungs at E18. Since a degree of alveolar simplification persists in the adult HER4$^{heart-/-}$ lungs [14], we speculate that the overall catch-up in progression of lung morphogenesis is not completed at the end of structural lung development in these animals. The murine fetal lung develops morphologically in 4 distinct stages, the pseudoglandular (E9.5–E16.5), the canalicular (E16.5–17.5), the saccular (E17.5–P5) and the alveolar (P5-30) stage [20]. The short duration at the canalicular stage makes the murine model at this gestation very useful for studying the effects of gene deletion on the progression of fetal lung morphogenesis. A similar histological picture is present in fetal mouse lungs lacking tumor necrosis factor-α converting enzyme (TACE). TACE plays a central role in the cleavage and shedding of the ErbB4 ectodomain [21]. Morphologically TACE-deleted animals have immature lungs with decreased lung branching and increased thickness of pulmonary mesenchyme [22], similar to the changes in the ErbB4 deleted lungs, suggesting that the disruption of lung development may be related to an inhibition of ErbB4 function in these animals. Other knock out animal models are known for an arrest in the maturation of the surfactant system at the canalicular

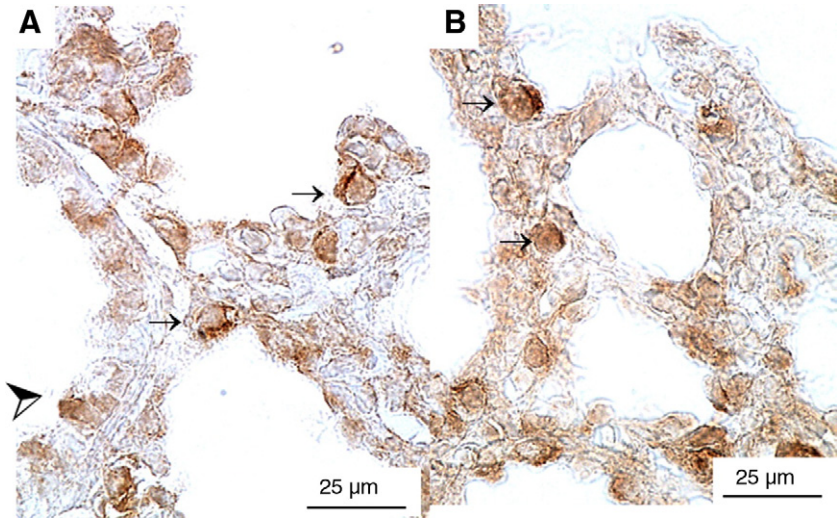

Fig. 4. Immunohistochemistry of SP-B protein expression in E18 control HER4$^{heart+/-}$ (A) and HER4$^{heart-/-}$ (B) fetal lungs. Representative images of lung sections from HER4$^{heart-/-}$ lungs (B) compared with HER4$^{heart+/-}$ control lungs (A). Dark brown staining is seen in SP-B-positive cells which include type II epithelial (small arrows) and Clara cells (large arrow head).

stage of lung development, e.g. in mice missing the gene for parathyroid hormone-related protein (PTHrP). Fetal and newborn PTHrP(−/−) lungs show delayed mesenchyme–epithelial interactions leading to an arrested type II cell differentiation and a disrupted development of the pulmonary surfactant system [23]. These similarities in the phenotype in PTHrP and ErbB4 (−/−) lungs are consistent with the observations that ErbB receptor signaling may regulate PTHrP gene expression in various epithelial cells. For example, the epidermal growth factor (EGF) receptor activates PTHrP gene expression in human keratinocytes [24] and EGF activates PTHrP gene expression in various types of epithelial cells [25,26].

At E18, the structure of ErbB4-deleted fetal lungs showed evidence of catch-up maturation with progression into the saccular stage. The observation of this catch-up structural development in HER4$^{heart-/-}$ lungs at E18 suggests the activation of compensatory mechanisms to correct for the missing function of ErbB4. Those mechanisms might include the participation of other ErbB receptors. The potential role of compensatory signaling by the remaining ErbB receptors is much more complex than a simple evaluation of receptor protein amounts. Overall baseline expression of the remaining ErbB4 receptors appears unchanged (work in progress), but distinct changes in dimer formation, receptor phosphorylation patterns, specific signaling, and receptor fate might be involved. ErbB2 is the ErbB receptor predominantly involved in direct interactions with other proteins [27–29], and would be a likely candidate for involvement in a compensatory process. Other signaling pathways such as the PTHrP pathway, known for its interaction with the EGFR [24–26] might also be involved. Further detailed studies are needed to elucidate these compensatory mechanisms.

Adult HER4$^{heart-/-}$ animals show signs of airway hyperreactivity and an underlying chronic inflammation [14]. This inflammation may have in part contributed to the pulmonary morphometric abnormalities seen in those adult animals. In this study we found that the late gestation fetal lungs already showed increased numbers of inflammatory cells. Based on this, we propose that there is an underlying abnormality in regulation of development of the lung inflammatory system in these ErbB4-deleted lungs.

Fetal ErbB4 deletion led to decreased surfactant phospholipid synthesis and delayed SP-B expression. The normalization of SP-B expression in the adult animals [14] is consistent with the observation that homozygous negative animals can survive without postnatal symptoms of surfactant deficiency and indicates a possible catch-up in the development of the surfactant system in association with the catch-up in morphologic development. In contrast to SP-B deficiency, the persistent change of SP-D protein expression in adulthood [14] may contribute to the increased numbers of inflammatory cells in the fetal lung, demonstrating a role of SP-D in the developmental control of lung immunity [30,31]. SP-D is a member of the collectin family with immunoregulatory functions [32]. An increased number of inflammatory cells in HER4$^{heart-/-}$ lungs is indicative of abnormal regulation of pulmonary immune development in the ErbB4-deleted lungs. In the fetal lung this led to an upregulation of SP-D mRNA, but not the SP-D protein. This is an obvious disconnect between the

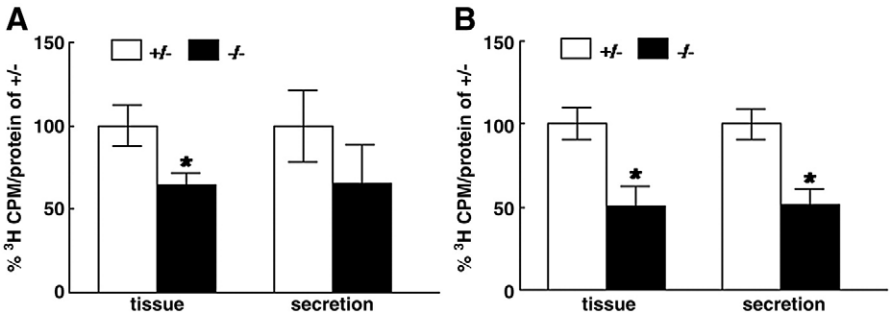

Fig. 5. DSPC synthesis (left group) and secretion (right group) in E17 (A) and E18 (B) fetal lung homogenates from HER4$^{heart+/-}$ (white bars) and HER4$^{heart-/-}$ (black bars) transgenic mice. Values are presented as mean ± SEM, $N = 4–14$, *: $p<0.05$.

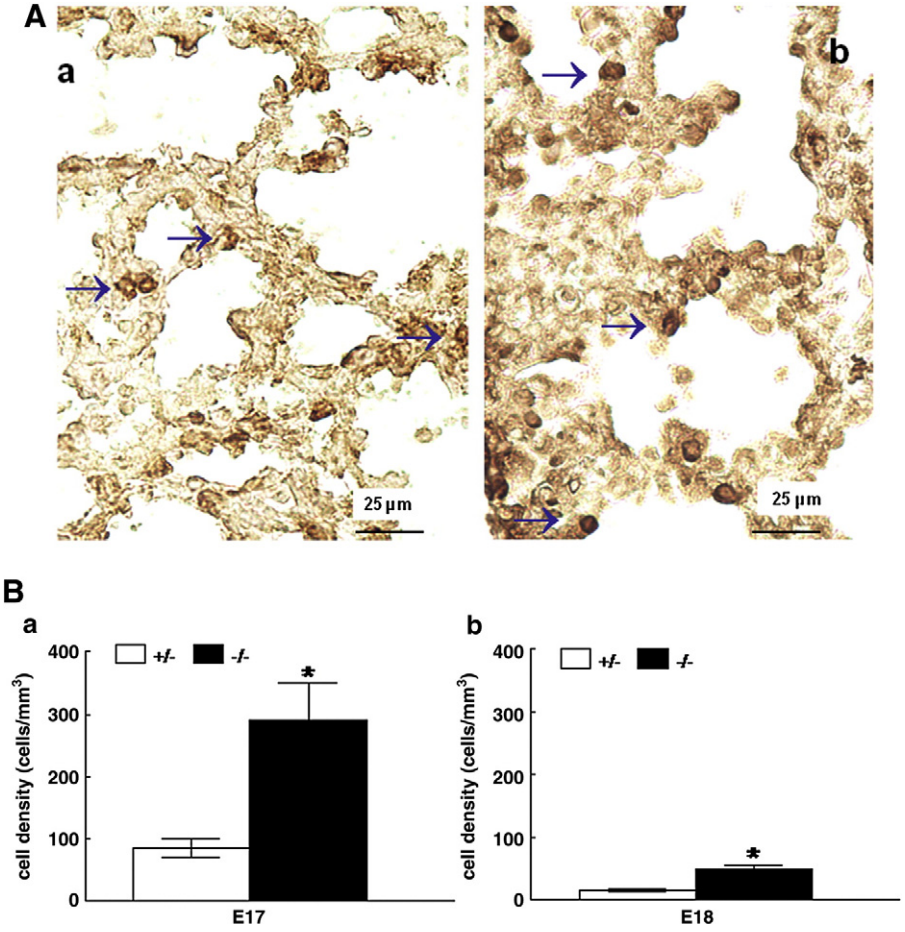

Fig. 6. A: Representative immunohistochemical images of CD11b expression in E18 control HER4$^{heart+/-}$ (a) and HER4$^{heart-/-}$ (b) fetal lung sections. Arrows indicate CD11b-positive cells, which are more frequently seen in HER4$^{heart-/-}$ lungs. B: Quantification of cell density (cells/mm^2) of CD11b positive cells in E17 (a) and E18 (b) fetal HER4$^{heart-/-}$ lungs (black bars) compared with HER4$^{heart+/-}$ control lungs (white bars). Values are presented as mean ± SEM, $N=7$, *: $p<0.05$.

protein and RNA level. The upregulation of SP-D mRNA in the fetal lung might be viewed as an attempt to appropriately regulate the development of lung immunity. The reason that the increased SP-D mRNA is not reflected in an increase in protein is not clear. It may reflect a block in transcription or an increased turnover of the protein in the fetal lungs. In adult HER4$^{heart-/-}$ animals, signs of chronic inflammation persist, but SP-D protein and mRNA expression are significantly downregulated [14], suggesting a burn out phenomenon of the RNA upregulation later in life.

Taken together, the findings of affected morphologic development in these animals are similar to a BPD-like picture observed in premature lambs after antenatal exposure to corticosteroids or cytokines [33,34]. Prenatal inflammation is an important triggering event in the pathogenesis of BPD [35], although the exact mechanisms are unknown. *In vitro* experiments show that glucocorticoid treatment promotes the maturation of the surfactant system [7] and simultaneously changes the expression and dimerization pattern of ErbB receptors in fetal type II cells from a prominent role of ErbB4 towards prominence of ErbB2 signaling [10]. Antenatal glucocorticoid administration improves lung maturation and prevents RDS in preterm infants [36], but the benefits coincide with an inhibition of alveolar development. The facts that glucocorticoids alter ErbB signaling in fetal lungs and that the anatomic structural changes in the glucocorticoid-treated lungs [33] are similar to those we have identified in fetal and adult ErbB4-deleted lungs [14] suggest that ErbB receptor dysregulation [10] might mediate some of the glucocorticoid effects on developing lung morphogenesis. Reduced branching and increased mesenchymal area around airspaces, as well as disrupted surfactant composition and function in the lungs of HER4$^{heart-/-}$ mice confirms the important role of ErbB4 receptors for the regulation of a timely progression of lung development. Our results suggest that the ErbB4 receptor is critical for a timely transition from the canalicular to saccular stage. This is not surprising since ErbB4 is well known for its role in the timely onset of other maturational processes including puberty [37] and the control of astrogenesis [38]. A loss of ErbB4 function may partially be rescued by compensatory mechanisms that likely include changes in the expression, dimerization patterns and receptor phosphorylation of the other three ErbB receptors. The fact that compensatory mechanisms exist suggests the basic importance of ErbB4 for normal lung development, as evolutionary mechanisms have been developed to compensate for its possible loss. This transgenic ErbB4 mouse model might be useful in studying the pathogenesis and treatment of neonatal lung disease.

Acknowledgements

We would like to thank Drs. M. Gassmann and C. Birchmeier for providing the HER4^{heart} mouse line. We are grateful to C. Acevedo, S. Rozek, and Dr. D. Wedekind for their assistance in animal experiments, breeding and genotyping.

This work is supported by a German Research Foundation (DFG) Grant Da 378/3-1 and Da 378/3-2, Gerber Foundation, Peabody Foundation, Susan B. Saltonstall Funds, and NIH HL-04436 and HL-037930, Tufts Medical Center Institutional Grant.

References

[1] D. Meyer, C. Birchmeier, Multiple essential functions of neuregulin in development, Nature 378 (1995) 386–390.
[2] M. Gassmann, F. Casagranda, D. Orioli, H. Simon, C. Lai, R. Klien, G. Lemke, Aberrant neural and cardiac development in mice lacking the ErbB4 neuregulin receptor, Nature 378 (1995) 390–394.
[3] K.F. Lee, H. Simon, H. Chen, B. Bates, M.C. Hung, C. Hauser, Requirement for neuregulin receptor erbB2 in neural and cardiac development, Nature 378 (1995) 394–398.
[4] D. Riethmacher, E. Sonnenberg-Riethmacher, V. Brinkmann, T. Yamaai, G.R. Lewin, C. Birchmeier, Severe neuropathies in mice with targeted mutations in the ErbB3 receptor, Nature 389 (1997) 725–730.
[5] W. Liu, K. Zscheppang, S. Murray, H.C. Nielsen, C.E. Dammann, The ErbB4 receptor in fetal rat lung fibroblasts and epithelial type II cells, Biochim. Biophys. Acta 1772 (2007) 737–747.
[6] H.C. Nielsen, Epidermal growth factor influences the development clock regulating maturation of the fetal lung fibroblast, Biochim. Biophys. Acta 1012 (1989) 201–206.
[7] C.E. Dammann, H.C. Nielsen, K.L. Carraway, Role of neuregulin1{beta} in the developing lung, Am. J. Respir. Crit. Care Med. 167 (2003) 1711–1716.
[8] C.E. Dammann, H.C. Nielsen, Regulation of the epidermal growth factor receptor in fetal rat lung fibroblasts during late gestation, Endocrinology 139 (1998) 1671–1677.
[9] C.E. Dammann, S.R. Ramadurai, D. McCants, L.D. Pham, H.C. Nielsen, Androgen regulation of signaling pathways in late fetal mouse lung development, Endocrinology 141 (2000) 2923–2929.
[10] C.E. Dammann, N. Nassimi, W. Liu, H.C. Nielsen, ErbB receptor regulation by dexamethasone in mouse type II epithelial cells, Eur. Respir. J. 28 (2006) 1117–1123.
[11] K. Zscheppang, E. Korenbaum, W. Bueter, S.M. Ramadurai, H.C. Nielsen, C.E. Dammann, ErbB receptor dimerization, localization, and co-localization in mouse lung type II epithelial cells, Pediatr. Pulmonol. 41 (2006) 1205–1212.
[12] K. Zscheppang, W. Liu, M.V. Volpe, H.C. Nielsen, C.E. Dammann, ErbB4 regulates fetal surfactant phospholipid synthesis in primary fetal rat type II cells, Am. J. Physiol. Lung Cell. Mol. Physiol. 293 (2007) L429–L435.
[13] H. Tidcombe, A. Jackson-Fisher, K. Mathers, D.F. Stern, M. Gassmann, J.P. Golding, Neural and mammary gland defects in ErbB4 knockout mice genetically rescued from embryonic lethality, PNAS 100 (2003) 8281–8286.
[14] E. Purevdorj, K. Zscheppang, H.G. Hoymann, A. Braun, D. von Mayersbach, M.J. Brinkhaus, A. Schmiedl, C.E. Dammann, ErbB4 deletion leads to changes in lung function and structure similar to bronchopulmonary dysplasia, Am. J. Physiol. Lung Cell. Mol. Physiol. 294 (2008) L516–L522.
[15] E.R. Weibel, Morphometry of the human lung: the state of the art after two decades, Bull. Eur. Physiopathol. Respir. 15 (1979) 999–1013.
[16] R.P. Bolender, D.M. Hyde, R.T. Dehoff, Lung morphometry: a new generation of tools and experiments for organ, tissue, cell, and molecular biology, Am. J. Physiol. 265 (1993) L521–L548.
[17] A. Schmiedl, M. Ochs, C. Muhlfeld, G. Johnen, F. Brasch, Distribution of surfactant proteins in type II pneumocytes of newborn, 14-day old, and adult rats: an immunoelectron microscopic and stereological study, Histochem. Cell Biol. (2005) 1–12.
[18] M. Amato, K. Petit, H.H. Fiore, C.A. Doyle, I.D. Frantz III, H.C. Nielsen, Effect of exogenous surfactant on the development of surfactant synthesis in premature rabbit lung, Pediatr. Res. 53 (2003) 671–678.
[19] T. Skripuletz, A. Schmiedl, J. Schade, S. Bedoui, T. Glaab, R. Pabst, S. von Horsten, M. Stephan, Dose-dependent recruitment of CD25+ and CD26+ T cells in a novel F344 rat model of asthma, Am. J. Physiol. Lung Cell. Mol. Physiol. 292 (2007) L1564–L1571.
[20] D. Warburton, M. Schwarz, D. Tefft, G. Flores-Delgado, K.D. Anderson, W.V. Cardoso, The molecular basis of lung morphogenesis, Mech. Dev. 92 (2000) 55–81.
[21] M. Vecchi, G. Carpenter, Constitutive proteolysis of the ErbB-4 receptor tyrosine kinase by a unique, sequential mechanism, J. Cell Biol. 139 (1997) 995–1003.
[22] J. Zhao, H. Chen, J.J. Peschon, W. Shi, Y. Zhang, S.J. Frank, D. Warburton, Pulmonary hypoplasia in mice lacking tumor necrosis factor-alpha converting enzyme indicates an indispensable role for cell surface protein shedding during embryonic lung branching morphogenesis, Dev. Biol. 232 (2001) 204–218.
[23] L.P. Rubin, C.S. Kovacs, M.E. De Paepe, S.W. Tsai, J.S. Torday, H.M. Kronenberg, Arrested pulmonary alveolar cytodifferentiation and defective surfactant synthesis in mice missing the gene for parathyroid hormone-related protein, Dev. Dyn. 230 (2004) 278–289.
[24] Y.M. Cho, D.A. Lewis, P.F. Koltz, V. Richard, T.A. Gocken, T.J. Rosol, R.L. Konger, D.F. Spandau, J. Foley, Regulation of parathyroid hormone-related protein gene expression by epidermal growth factor-family ligands in primary human keratinocytes, J. Endocrinol. 181 (2004) 179–190.
[25] J.K. Heath, J. Southby, S. Fukumoto, L.M. O'Keeffe, T.J. Martin, M.T. Gillespie, Epidermal growth factor-stimulated parathyroid hormone-related protein expression involves increased gene transcription and mRNA stability, Biochem. J. 307 (Pt 1) (1995) 159–167.
[26] S.L. Ferrari, R. Rizzoli, J.P. Bonjour, Effects of epidermal growth factor on parathyroid hormone-related protein production by mammary epithelial cells, J. Bone Miner. Res. 9 (1994) 639–644.
[27] A. Eisenberg, E. Biener, M. Charlier, R.V. Krishnan, J. Djiane, B. Herman, A. Gertler, Transactivation of erbB2 by short and long isoforms of leptin receptors, FEBS Lett. 565 (2004) 139–142.
[28] A. Ray, K.J. Nkhata, M.P. Cleary, Effects of leptin on human breast cancer cell lines in relationship to estrogen receptor and HER2 status, Int. J. Oncol. 30 (2007) 1499–1509.
[29] S.E. Seton-Rogers, Y. Lu, L.M. Hines, M. Koundinya, J. LaBaer, S.K. Muthuswamy, J.S. Brugge, Cooperation of the ErbB2 receptor and transforming growth factor beta in induction of migration and invasion in mammary epithelial cells, Proc. Natl. Acad. Sci. USA 101 (2004) 1257–1262.
[30] C. Botas, F. Poulain, J. Akiyama, C. Brown, L. Allen, J. Goerke, J. Clements, E. Carlson, A.M. Gillespie, C. Epstein, S. Hawgood, Altered surfactant homeostasis and alveolar type II cell morphology in mice lacking surfactant protein D, Proc. Natl. Acad. Sci. USA 95 (1998) 11869–11874.
[31] T.R. Korfhagen, V. Sheftelyevich, M.S. Burhans, M.D. Bruno, G.F. Ross, S.E. Wert, M. T. Stahlman, A.H. Jobe, M. Ikegami, J.A. Whitsett, J.H. Fisher, Surfactant protein-D regulates surfactant phospholipid homeostasis in vivo, J. Biol. Chem. 273 (1998) 28438–28443.
[32] J.R. Wright, Immunoregulatory functions of surfactant proteins, Nat. Rev. Immunol. 5 (2005) 58–68.
[33] G.R. Polglase, I. Nitsos, A.H. Jobe, J.P. Newnham, T.J. Moss, Maternal and intra-amniotic corticosteroid effects on lung morphometry in preterm lambs, Pediatr. Res. 62 (2007) 32–36.
[34] K.E. Willet, B.W. Kramer, S.G. Kallapur, M. Ikegami, J.P. Newnham, T.J. Moss, P.D. Sly, A.H. Jobe, Intra-amniotic injection of IL-1 induces inflammation and maturation in fetal sheep lung, Am. J. Physiol. Lung Cell. Mol. Physiol. 282 (2002) L411–L420.
[35] A.H. Jobe, E. Bancalari, Bronchopulmonary dysplasia, Am. J. Respir. Crit. Care Med. 163 (2001) 1723–1729.
[36] D. Roberts, S. Dalziel, Antenatal corticosteroids for accelerating fetal lung maturation for women at risk of preterm birth, Cochrane Database Syst. Rev. 3 (2006) CD004454.
[37] V. Prevot, C. Rio, G.J. Cho, A. Lomniczi, S. Heger, C.M. Neville, N.A. Rosenthal, S.R. Ojeda, G. Corfas, Normal female sexual development requires neuregulin-erbB receptor signaling in hypothalamic astrocytes, J. Neurosci. 23 (2003) 230–239.
[38] S.P. Sardi, J. Murtie, S. Koirala, B.A. Patten, G. Corfas, Presenilin-dependent ErbB4 nuclear signaling regulates the timing of astrogenesis in the developing brain, Cell 127 (2006) 185–197.